Mon. Not. R. Astron. Soc. **274,** 491–498 (1995)

A search for stellar aggregates in dwarf spheroidal galaxies

Serge Demers,[1]★ Paolo Battinelli,[2] M. J. Irwin[3]★ and W. E. Kunkel[4]

[1] *Département de Physique and Observatoire du mont Mégantic, Université de Montréal, Montréal, Canada H3C 3J7*
[2] *Osservatorio Astronomico di Roma, viale del Parco Mellini 84, I-00136 Roma, Italy*
[3] *Royal Greenwich Observatory, Madingley Road, Cambridge CB3 0EZ*
[4] *The Observatories of the Carnegie Institution of Washington, La Serena, Chile*

Accepted 1994 December 13. Received 1994 December 8; in original form 1994 September 5

ABSTRACT

We use the Path-Linkage-Criterion (PLC) technique to identify aggregates of stars in the dwarf spheroidal galaxies Leo I, Leo II, Fornax, Draco and Ursa Minor. The PLC technique is calibrated by applying it to random distributions of points matching the observed global two-dimensional surface density distributions of the five galaxies. Comparison of these results shows that stars are locally distributed at random in four of these dwarf spheroidals under study, and no aggregates of stars, above the noise, are identified (excluding the obvious globular clusters). Special attention is given to the putative cluster 6 of Fornax, which we can explain as a random fluctuation of the stellar surface density.

Deep CCD data of the central regions of Ursa Minor and Draco are used to place limits on possible massive black holes in these systems. No excess of stars is found in the centre of Draco, giving a limit on any central black hole of $< 3 \times 10^5\ M_\odot$. For Ursa Minor, a non-random clump of stars is identified near the centre of the galaxy. If this clump were the signature of a black hole, as postulated by Strobel & Lake, the black hole mass would be less than $\sim 10^6\ M_\odot$. This is insufficient to explain the apparently high mass-to-light ratio of Ursa Minor, but significant enough to warrant further investigation.

Key words: galaxies: individual: Leo I – galaxies: individual: Leo II – galaxies: individual: Fornax – galaxies: individual: Draco – galaxies: individual: Ursa Minor – galaxies: star clusters.

1 INTRODUCTION

It is now recognized that the evolutionary history of dwarf spheroidal galaxies surrounding the Milky Way is rather complex. In contrast to the globular clusters, the stellar populations of dwarf spheroidal galaxies show a marked diversity in age. At one extreme, Ursa Minor (Olszewski & Aaronson 1985) contains only stars older than ~16 Gyr, whereas the bulk of the stellar populations of Carina (Mould & Aaronson 1983; Mighell 1990), Leo I (Lee et al. 1993; Demers, Irwin & Gambu 1994a) and Fornax (Demers, Irwin & Kunkel 1994b) are younger than 6 Gyr. Whilst it is tempting to treat the Galactic dwarf spheroidals as isolated systems, it is very likely that tidal interactions play an important role in their evolutionary history. The presence of the Magellanic Stream in the wake of the Large Magellanic Cloud is proof that tidal interaction plays a role in the vicinity of the Milky Way. For dwarf spheroidals no gas tails are observed, but the asymmetric isophotes of Fornax (Demers et al. 1994b) and the truncated profile of Saggitarius (Ibata, Gilmore & Irwin 1994) support this view. Furthermore, certain spheroidals, close to the Galactic pole, are elongated in a direction consistent with a polar orbit.

According to current models of galaxy formation, a galaxy like the Milky Way grew initially from a high primordial density fluctuation, on to which merged over time the evolutionary results of a large number of smaller, or satellite, density fluctuations (e.g. Silk & Wyse 1993). In this scenario, typical 1σ fluctuations resulted in dwarf-galaxy-sized perturbations that either evolved into dwarf galaxies, interacted with each other, or were incorporated into the Milky Way. The apparent non-random spatial distribution of the Galac-

★ Visiting Observers, Canada–France–Hawaii Telescope, operated by the National Research Council of Canada, le Centre National de la Recherche Scientifique de France and the University of Hawaii.

tic dwarf satellites and the recent discovery of the distended Sagittarius dwarf galaxy close to the Galactic Centre (Ibata et al. 1994) lend support to this picture. The close spatial proximity of the orbital plane of the Magellanic Clouds to the majority of the Galactic dwarf spheroidals has even led to the suggestion that some dwarf spheroidals may be stripped tidal remnants of close interactions between the Magellanic Clouds and the Milky Way (Kunkel 1979; Lynden-Bell 1982; Majewski 1993). Tidal shocks would have influenced the internal stellar distribution and subsequent stellar evolution of those systems (Lynden-Bell 1967). Alternatively, Faber & Lin (1983) speculated that the Galactic dwarf spheroidals could be the remnants of stripped dwarf irregular galaxies. In this scenario the distribution of intermediate-age star formation sites might be expected to show some signature of the irregular structure of the precursor system.

With systemic star–star relaxation times for the dwarf spheroidals much greater than a Hubble time we might therefore expect to find evidence of such tidal interactions, or evolutionary relics, in their stellar density distributions. However, as noted by Lynden-Bell (1967), the influence of a time-varying Galactic potential can act to give well-mixed star distributions in far less than a Hubble time.

To our knowledge no systematic study has been made of dwarf spheroidal star distributions, but evidence of non-random star distributions has been claimed in a few systems: Sculptor (Eskridge 1988a), Fornax (Eskridge 1988b) and Ursa Minor (Olszewski & Aaronson 1985). Indeed, the apparent high mass-to-light ratios of Draco and Ursa Minor lead Strobel & Lake (1994) to suggest that a black hole of $\sim 10^7\,M_\odot$ may be located in their core. Such black holes would enhance the local stellar density near the centre, which in turn should lead to the presence of a cusp in the observed surface density profile and a significant increase in velocity dispersion near the centre.

In order to examine the hypothesis of putative black holes in Draco and Ursa Minor and to investigate further the presence or otherwise of non-random star distributions in the Galactic dwarf spheroidals, we present results of an investigation into those dwarf spheroidals for which we have available deep astrometry and photometry. We have based the analysis on the automated technique developed by Battinelli (1991) and apply this method to the two-dimensional distribution of stars in Fornax, the most massive spheroidal, Leo I and Leo II, the most distant Galactic spheroidals, and Ursa Minor and Draco, the two smallest systems with the highest apparent mass-to-light ratios.

2 The DATA BASE

For Leo I and Leo II we use CCD frames obtained at the prime focus of the Canada–France–Hawaii 3.6-m telescope. The 2048×2048 CCD employed corresponds to a field of 7×7 arcmin^2, sufficient to include most of these two galaxies. The data base for Leo I consists of 3475 giant stars, brighter than $V=22.0$, observed by Demers et al. (1994a). Leo II is less populous than Leo I; here we have 2200 stars taken from the published photometry of Demers & Irwin (1993). The reduced CCD data consist of files with x, y coordinates, magnitudes and colours.

In the case of Fornax, we select a subsample of the data base of Demers et al. (1994b). This data base consists of 97 000 stars, for which we have x, y coordinates, magnitudes and colours, identified by the APM on a prime-focus CTIO 4-m sky-limited IIIa-J plate. For our current study of the field of Fornax, we analyse the distribution of a subset of ~ 5500 giants, to a limiting magnitude of $V=19.7$. The selection of a subset of this size is required by the PLC technique, which is impractical to run with extremely large data sets. Fig. 1 presents the field of the CTIO 4-m plate and the 5500 stars. Cluster 2 is seen south-west of the centre, and cluster 3 is less obvious at $x=-3000$, $y=-5500$. Stars in and near clusters 2 and 3 have been excluded from the analysis. For the study of the ill-defined cluster 6 (Hodge & Smith 1974) we do not restrict the sample to bright stars, but select all the stars from the data base in an area 1000×1000 units centred on cluster 6.

The Draco and Ursa Minor data were obtained with the Isaac Newton telescope, on La Palma, in 1994 May. A 1240×1140 thick, coated EEV CCD was employed, with a scale of 0.55 arcsec per pixel, corresponding to a field of view of 11×10 arcmin^2. A single 900-s R-band frame was taken of Draco, centred on the galaxy, which reaches an apparent magnitude of $R\approx24$. This single frame was sufficient to cover the main central part of the galaxy. Ursa Minor, however, is more elongated, and the central region of interest subtends some 20 arcmin of sky. Consequently, two overlapping frames, 900-s R-band CCD frames with a limiting magnitude of $R\approx24$, were used to cover this region. Frame 1 is centred at RA$=15^h7^m50^s$, Dec.$=+67°21'0''$. Frame 2 is centred at RA$=15^h8^m56^s$, Dec.$=+67°29'0''$ (B1950). The Draco file contains 5400 stars, while the two Ursa Minor files contain 4000 and 3400 stars respectively. The two Ursa Minor frames overlap in an area of roughly 300×500 pixel. These two files were merged before the analysis of the star distribution was done.

3 RESULTS

3.1 The technique

The Path-Linkage-Criterion technique requires the determination of a scalelength d_s, a parameter which is function of the surface density of the field. The underlying algorithm is that star a and star b will be assigned to the same group if it is possible to go from a to b, jumping from star to star in steps smaller than d_s. It is important to note that the agglomerative algorithm is able to detect compact and filamentary groups but will not, in general, be optimized for detecting large-scale asymmetries, such as that observed in Fornax by Demers et al. (1994b).

The determination of d_s is done through the function $f_p(d)$, which represents the number of clumps containing at least p stars identified using a value d as scalelength. When the critical value of d is reached, $f_p(d)$ reaches a plateau or a maximum depending on the average population within each group compared to the total population. The value of d_s is set as this critical value of d. Further details of the technique are given in Battinelli (1991) and Battinelli & Demers (1992).

The application of the PLC technique to spheroidal galaxies having radial stellar density gradients requires some modifications. The galaxies were divided in elliptical annuli, of approximately constant surface density, and a d_s was determined for each annulus. Thus, to each point in the field

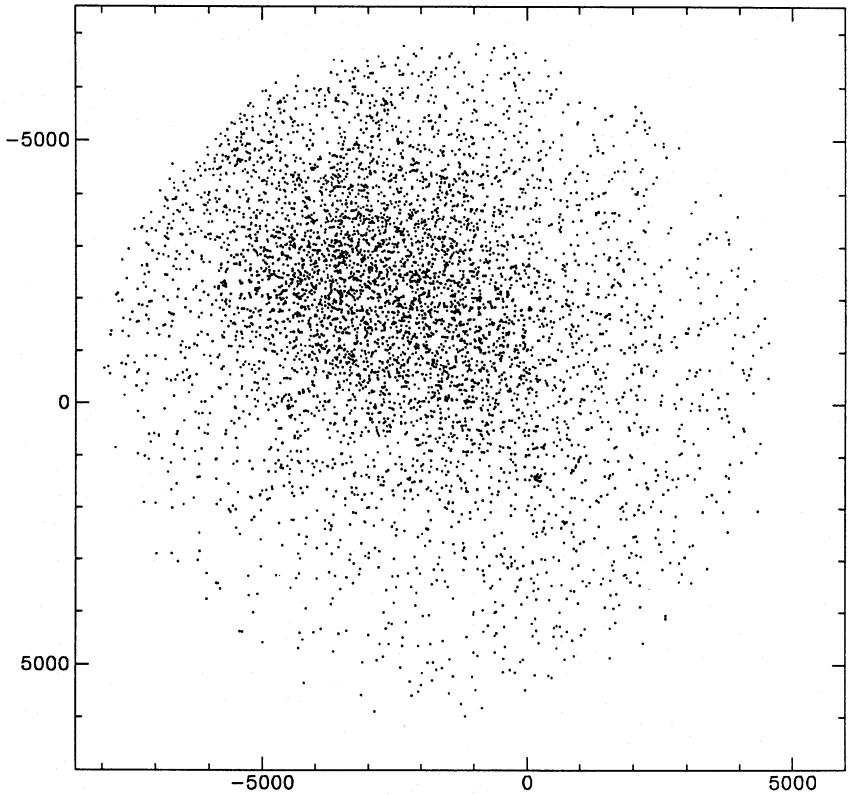

Figure 1. Map of the 5500 giant branch stars of Fornax seen in the CTIO prime-focus field. North is at the top, east to the left; 1000 units correspond to 4.71 arcmin.

one can assign a d_s by interpolation from the values in the annuli. The PLC technique is then applied to the whole galaxy, using a variable d_s. The five galaxies under investigation present different levels of complexity. Draco and Ursa Minor have a low, rather uniform stellar density. Leo II has circular symmetry, Leo I a constant elliptical symmetry, and Fornax a variable elliptical symmetry with evidence of non-elliptical distortions.

Our approach to the search for non-random clumps or filaments of stars consists in first identifying groups of stars using the PLC method on the actual data, and then to compare these with the PLC technique applied to randomly generated star distributions. The generated random distributions have the same surface density and the same d_s as the annulus under comparison.

3.2 Statistical tests

Given a suspected non-random distribution of stars, we then need to define a suitable statistical measure, or hypothesis test, to quantify the probability of finding such an occurrence by chance. The null hypothesis is that the dwarf spheroidals have essentially random distributions of stars, governed by some overall smooth profile. There are several possible statistical tests that one could apply to check the hypothesis. The simplest, conceptually, would be to run sufficient Monte Carlo simulations such that for any value of d_s for a particular object the frequency distribution of numbers of clumps for the equivalent random distribution could be calibrated. However, since the probability of locating, say, r PLC clumps for a fixed surface density of objects depends in general on the combined effects of many random variables, we might expect that the underlying clump distribution $P(r)$ is governed by the Central Limit Theorem. If so, $P(r)$ should approximately follow a Poisson distribution, tending to a Gaussian for large values of the expected number of clumps, a. In other words, the probability of observing r clumps when you expect a mean of a is

$$P(r)=\frac{a^r \exp(-a)}{r!},$$

and the probability of seeing r or more clumps in random data is then simply

$$P(\geq r)=1-\sum_{i=0}^{i=r-1}\frac{a^r \exp(-a)}{r!}.$$

For the rare clusters or large associations the probability of getting one by chance is just $1-\exp(-a)$.

We tested the reliability of this approximation using detailed Monte Carlo simulations (100 trials) using the Ursa Minor surface density. In all cases covering the range of N_{star} from three or more stars per clump up to 100 or more per clump the Poisson distribution provided a good detailed fit to the Monte Carlo simulated distribution. This enables us to speed up the simulations by a factor of 10 or more, since all we now need to know is the expected mean number of clumps (i.e. a) for a given N_{star}. We note that a Kolmogorov–Smirnov (KS) test applied directly to the observed and

expected means would be insensitive to the presence of one or two big clumps of stars. The KS test is more sensitive to subtle ordered global variations in number distributions.

3.3 Leo I

Because of its distance from the Milky Way, Leo I appears compact. We adopt, for Leo I, the distance of 205 kpc determined by Demers et al. (1994a) and the ellipticity of $\varepsilon = 0.21$ and the major-axis orientation of $\theta = 79°$ determined by Irwin & Hatzidimitriou (1993). The galaxy was divided into six annuli of width 200 pixel, corresponding to 41 arcsec, and the PLC was applied to each annulus with the usual procedure to determine d_s for each annulus. Once the d_s are known, the PLC is applied to the whole galaxy.

Random distributions were obtained so that the number of stars was equal to the number observed in each annulus. Table 1 presents the comparison between the results of the observed distributions of clumps and the randomly produced ones. We list the number of clumps containing N_{star} or more stars for the observed data and the random data, an average of five random distributions (numbers given between parentheses). The last two lines of the table give the d_s, in arcsec and pc, adopted for each annulus. In no case is there compelling evidence for any departure from randomness of the stellar distribution. We caution against overinterpreting individual probabilities (using the Poisson approximation), since the tables contain many semi-independent attempts to detect clumps or aggregates of stars.

3.4 Leo II

Leo II is less dense than Leo I and has fewer stars than Leo I. Because its ellipticity is zero, we use six circular rings. The procedure is the same as that applied to Leo I. For this galaxy we adopt the distance of 215 kpc determined by Demers & Irwin (1993). As can be seen by the inspection of Table 2, the results of the real and random distributions are nearly identical, with no evidence of stellar clustering. Here again the adopted d_s are given in the last two lines.

3.5 Fornax

Fornax has a rather chaotic inner structure (Demers et al. 1994b). We have divided the area into nine elliptical annuli corresponding roughly to the observed structure of Fornax. The exact value of the ellipticity and orientation of each annulus does not have to match perfectly the structure of Fornax. We simply need areas with uniform stellar surface densities. Tests could have been done by dividing Fornax into a multitude of 5×5 arcmin^2 cells. A circular area around cluster 3 and cluster 2 was removed from the data base. Cluster 4, in the central part, is so compact that very few of its giants are in our file.

Table 3 gives the comparison between the observed distributions and the one obtained from the average of five random tests. Again we see that there is little difference between the observed distribution and the random distribution, apart from the innermost annulus where there is a tendency for a larger number of PLC clumps to be present than expected. This region corresponds to the central distorted elliptical isophotes noted by Demers et al. (1994b), and we suspect that the differences here are caused by the true surface density varying more rapidly than our annular approximation. The characteristic lengths d_s, in arcsec and in pc, are listed in the last two lines of the table.

3.6 Cluster 6 of Fornax

Ever since the early studies of Fornax, investigators have noticed a fuzzy patch of stars north of cluster 4. Indeed, Hodge (1961a) writes that Shapley mentioned, following his discovery of Fornax, a faint object just 7 arcmin north of cluster 4. Hodge states that on a 200-inch plate, taken by

Table 1. Leo I: comparison between observed and random distributions.

N_{star}	ann. 1	ann. 2	ann. 3	ann. 4	ann. 5	ann. 6
3	16 (17.2)	44 (47.0)	57 (50.4)	65 (50.2)	36 (38.4)	15 (9.0)
4	9 (10.2)	29 (31.6)	32 (33.4)	48 (35.4)	28 (26.0)	11 (4.0)
5	8 (7.2)	22 (21.8)	22 (24.2)	39 (28.4)	18 (17.6)	7 (3.4)
6	6 (4.6)	17 (17.0)	15 (18.6)	33 (22.0)	12 (13.0)	3 (2.0)
7	4 (3.0)	14 (13.2)	13 (14.4)	26 (17.2)	9 (9.4)	3 (1.6)
8	2 (2.2)	10 (9.2)	10 (12.0)	18 (13.2)	7 (7.0)	2 (0.8)
9	2 (1.0)	7 (7.2)	8 (10.4)	14 (10.8)	5 (5.6)	2 (0.6)
10	0 (0.8)	6 (5.4)	7 (9.0)	8 (8.6)	4 (4.2)	1 (0.6)
11		6 (4.0)	5 (6.8)	8 (6.8)	2 (3.0)	1 (0.4)
12		4 (3.2)	3 (6.2)	5 (5.4)	1 (2.0)	1 (0.4)
13		2 (2.2)	2 (5.2)	4 (4.2)	1 (1.2)	1 (0.4)
14		2 (1.6)	2 (4.2)	3 (3.6)	0 (0.8)	1 (0.4)
15		2 (1.4)	2 (3.2)	2 (2.6)		1 (0.2)
16		2 (1.0)	2 (3.0)	1 (2.0)		1 (0.2)
17		0 (0.6)	2 (2.8)	0 (2.0)		1 (0.2)
18			2 (2.8)			0 (0.2)
19			2 (2.8)			
25			1(0.8)			
26			0(0.6)			
d_s''	3.8	4.6	5.6	6.7	7.8	10.6
$d_s(pc)$	4	5	6	7	8	11

Table 2. Leo II: comparison between observed and random distributions.

N_{star}	ring 1	ring 2	ring 3	ring 4	ring 5	ring 6
3	18 (18.2)	59 (53.6)	62 (67.0)	61 (63.4)	52 (46.0)	15 (12.6)
4	11 (10.2)	37 (34.6)	45 (43.4)	31 (40.4)	37 (30.8)	9 (8.2)
5	5 (6.6)	24 (24.0)	38 (33.0)	17 (28.2)	22 (19.4)	5 (3.2)
6	5 (4.4)	19 (16.8)	26 (25.4)	14 (19.8)	15 (12.2)	4 (1.8)
7	5 (2.4)	13 (12.6)	22 (21.2)	10 (14.4)	11 (9.4)	2 (1.0)
8	4 (1.8)	10 (9.4)	20 (16.6)	7 (10.2)	9 (6.4)	1 (0.6)
9	4 (1.4)	8 (6.4)	15 (13.2)	6 (7.6)	6 (4.6)	1 (0.6)
10	2 (0.4)	3 (4.2)	11 (9.4)	5 (5.2)	3 (2.4)	1 (0.2)
11	1 (0.2)	2 (3.6)	8 (7.6)	5 (4.4)	0 (1.2)	1 (0.2)
12	0 (0.0)	0 (2.6)	7 (6.8)	4 (2.8)		1 (0.2)
13			4 (5.8)	3 (1.8)		0 (0.0)
14			4 (5.2)	2 (1.4)		
15			4 (4.6)	2 (1.4)		
16			2 (3.0)	2 (1.2)		
21			1 (1.0)	1 (0.4)		
22			1 (0.4)	0 (0.2)		
25			1 (0.2)			
26			0 (0.0)			
d_s''	3.8	3.9	5.4	6.1	7.8	11.4
$d_s(pc)$	4	4	6	6	8	12

Table 3. Fornax: comparison between observed and random distributions.

N_{star}	ann. 1	ann. 2	ann. 3	ann. 4	ann. 5	ann. 6	ann. 7	ann. 8	ann. 9
3	70 (55.0)	142(134.0)	134(122.2)	112(101.2)	65(68.4)	36(46.8)	25(26.6)	39(37.6)	13(14.6)
4	44(33.2)	98(85.6)	97(81.4)	76(69.2)	40(44.4)	21(30.6)	18(16.4)	24(20.6)	4(7.6)
5	31(17.2)	64(57.6)	63(59.8)	49(49.8)	25(29.4)	16(21.8)	12(11.4)	19(12.4)	4(3.8)
6	23(10.8)	49(38.6)	49(42.6)	28(39.0)	19(21.0)	10(15.2)	9(7.8)	7(8.6)	3(2.8)
7	14(6.2)	33(26.8)	37(32.2)	19(28.0)	13(15.6)	5(11.8)	5(5.6)	3(5.6)	2(2.2)
8	8(2.6)	28(19.8)	32(26.6)	16(22.0)	10(11.6)	5(9.0)	5(3.6)	3(4.0)	2(2.0)
9	6(2.0)	19(14.6)	25(19.8)	14(18.2)	6(9.4)	2(7.8)	2(2.4)	2(2.8)	1(1.0)
10	6(1.4)	16(12.6)	24(15.6)	12(15.8)	4(7.4)	1(6.0)	2(2.2)	1(1.6)	0(0.4)
11	5(1.0)	13(11.2)	19(11.8)	8(13.8)	4(5.6)	1(4.4)	2(1.4)	1(1.2)	0(0.4)
12	4(0.6)	10(6.6)	15(9.0)	7(11.4)	4(4.6)	1(3.8)	2(1.4)	1(0.8)	0(0.2)
13	3(0.4)	7(5.4)	8(7.2)	6(10.6)	4(4.2)	0(3.2)	1(1.2)	0(0.4)	0(0.2)
14	3(0.2)	5(5.0)	7(6.8)	6(8.0)	2(4.0)	0(2.2)	0(1.2)	0(0.4)	0(0.2)
15	3(0.2)	5(4.0)	5(4.8)	5(6.8)	2(3.8)	0(1.6)	0(0.8)	0(0.2)	0(0.0)
16	2(0.2)	4(3.0)	4(4.0)	3(5.6)	1(3.0)	0(1.4)	0(0.6)	0(0.2)	0(0.0)
17	1(0.2)	3(2.8)	3(2.4)	3(4.8)	1(2.8)	0(1.2)	0(0.6)	0(0.2)	0(0.0)
18	1(0.2)	2(2.4)	2(1.6)	3(4.2)	1(2.6)	0(1.2)	0(0.4)	0(0.2)	0(0.0)
19	0(0.2)	1(1.6)	1(1.4)	2(3.8)	1(1.8)	0(1.2)	0(0.4)	0(0.2)	0(0.0)
20	0(0.2)	0(1.4)	1(1.2)	2(3.2)	0(1.6)	0(1.2)	0(0.4)	0(0.2)	0(0.0)
21	0(0.0)	0(1.4)	1(1.0)	1(2.8)	0(1.4)	0(1.2)	0(0.4)	0(0.2)	0(0.0)
22	0(0.0)	0(1.2)	0(1.0)	0(2.2)	0(1.4)	0(1.2)	0(0.4)	0(0.0)	0(0.0)
d_s''	11.9	15.5	20.7	25.1	32.7	42.1	44.4	55.1	61.7
$d_s(pc)$	8	10	13	16	21	27	28	35	39

Baade, this object appears as a group of five stars of approximately 21st magnitude. It is interesting to note, however, that Hodge (1961a) does not include this faint object among the globular clusters of Fornax. During the 1960s this feature eventually became known as cluster 6. Hodge (1969) stated that inspection of deep plates shows that it is a loose globular cluster similar to cluster 1. In Hodge's (1971) review of dwarf galaxies, Fornax is then described as having six globular clusters, and a few years later Hodge & Smith (1974) listed the coordinates of the six clusters of Fornax. Verner et al. (1981), in their photometric investigation of the globular clusters of Fornax, were unable to confirm that cluster 6 was indeed a genuine globular cluster. Recently, Demers et al. (1994b) show that cluster 6 contains barely half a dozen more giants than areas of the same size in the nearby field of Fornax. Furthermore, they state that the apparent size of cluster 6 is quite small for a supposed loose cluster.

In order to apply the PLC to the problem of cluster 6 we have selected, from the original data base, all the stars in an area of 4.3×4.3 arcmin^2 including cluster 6. This area contains slightly more than 2300 stars. The PLC technique yields a $d_s = 4.2$ arcsec corresponding to 3 pc. That this d_s is smaller than those found for Fornax itself reflects simply the higher stellar density of the data base selected. Comparisons with random distributions reveal that the enhancement of stars known as cluster 6 is likely to be a statistical artefact. The greatest deviation between the observed distribution and the random test is at the 6 per cent chance level. However, given the number of 'independent' degrees of freedom in the numbers, this is not significant. Cluster 6 is just a 1.5–2.0σ fluctuation.

3.7 Draco

Draco is much closer to the Galaxy than the previous three galaxies. Our CCD observation samples only its core. In this region the stellar surface density does not show a strong radial gradient. For this reason, the PLC technique was applied to the whole area without subdividing it. The comparison between our results on the observed data and the average of five random tests is presented in Table 4. We list the number of clumps containing $N_{\rm star}$ stars. The largest clump identified has 29 stars, but such clumps are also seen in the random tests. We thus conclude that there are no aggregates of stars in the central part of Draco. A distance of 76 kpc for Draco (Stetson 1979) was used in computing the d_s in pc.

Table 4. Draco: comparison between observed and random distributions.

N_{star}	observed	random
3	631	630.73
4	416	401.90
5	254	264.90
7	114	130.53
8	78	93.13
9	54	69.06
10	41	51.69
11	34	39.56
12	28	30.49
13	24	23.36
14	21	17.99
15	17	14.89
16	12	11.66
17	9	9.76
18	6	8.29
19	4	6.02
20	2	4.59
21	2	3.96
22	2	3.13
23	2	2.46
24	2	1.93
25	2	1.63
26	2	1.36
27	1	1.03
28	1	0.93
29	1	0.76
30	0	0.63
d_s''	6.37	
$d_s(pc)$	2.3	

Table 5. UMi: comparison between observed and random distributions.

N_{star}	observed	random
3	275	269.70
4	161	157.13
5	82	98.33
6	61	65.33
7	46	41.57
8	23	31.20
9	25	22.10
10	14	17.13
11	17	12.70
12	11	8.73
13	8	6.90
14	7	5.80
15	6	4.93
16	4	2.90
17	0	2.20
18	5	2.13
19	2	1.70
20	3	1.13
21	0	1.17
22	1	0.93
23	3	0.90
33	1	0.37
78	1	0.00
d_s''	7.8	
$d_s(pc)$	2.6	

3.8 Ursa Minor

Ursa Minor, like Draco, is close to the Galaxy. Nemec, Wehlau & Mendes de Oliveira (1988) quote a distance of 70 kpc for Ursa Minor. With a core radius of 15.8 arcmin (Irwin & Hatzidimitriou 1993), even with two CCD frames we sample only the core of Ursa Minor. Like Draco, the stellar radial density gradient is sufficiently low to permit the application of the PLC technique to the whole area without modification of the d_s. Comparison between the observed distribution and the distributions of the random tests, given in Table 5, shows one obvious difference. We see in the observed data a clump of 78 stars that is not at all expected from the random distribution (probability of $<10^{-5}$). This aggregate of stars coincides with the centre of Ursa Minor.

4 DISCUSSION

The dwarf spheroidal galaxies under investigation have experienced significantly different histories of star formation. The bulk of the stars of Leo I and Fornax are much younger than the Local Group, indicating that strong stellar formation activity took place a long time after the initial epoch of galaxy formation. The stellar populations of Leo II and of Draco are, however, more in line with the Local Group canonical age of 12 to 15 Gyr, even though the horizontal branch of Leo II shows the second-parameter syndrome (Demers & Irwin 1993). Ursa Minor is made up almost exclusively of old stars (Olszewski & Aaronson 1985). Neither Fornax nor Leo I shows any evidence of star formation at the present epoch, as seen, for example, in the Phoenix dwarf galaxy (van de Rydt, Demers & Kunkel 1991). Consequently, all of the dwarfs studied have had at least ~5 Gyr since their last major burst of star formation. Any stellar associations or clusters should therefore now be well mixed with their locale.

Since there is no evidence of any significant amounts of either H I gas or dust in any of the Galactic dwarf spheroidals (Knapp, Kerr & Browers 1978; Mould et al. 1990), any apparent overdensity or underdensity of stars will be real and not an artefact of differential obscuration. Assuming that sites of star formation have typical scalelengths comparable to Galactic stellar associations, ~100 pc in diameter, we can test the PLC technique to see if it would have detected such large structures. More specifically, we would like to investigate the presence or otherwise of large structures in Fornax. Eskridge (1988b) claimed to have identified such features in the residuals (raw counts – elliptically symmetric smooth distribution) of the two-dimensional stellar distribution of Fornax that measure ~200 pc in size. These surpluses of stars amount to 40 per cent of the surrounding field density. As an example, the artificial insertion of cluster 1 into the central Fornax region represents an increase of 32 per cent of the stellar density in a patch of 1 arcmin in diameter, or about 40 pc. The PLC could easily detect this addition of stars as a 'cluster'. Therefore the PLC technique should have identified the structures mentioned by Eskridge. The recent study of Fornax by Demers et al. (1994b) has shown that the internal structure of Fornax is much more complex than Eskridge assumed, showing large-scale asymmetries. The centre and the orientation of the isopleths vary significantly, suggesting that the residual structures noted by Eskridge are more likely to be artefacts caused by the assumption of local elliptical symmetry. We therefore conclude that the two-dimensional stellar distribution of Fornax does not show local irregularities which can be attributed to stellar aggregates, excluding, of course, the five globular clusters. However, Fornax does indeed show global irregularities in the inner isophotes (noted by Hodge 1961b) that could best be described as a distortion of the inner structure (Demers et al. 1994b).

The so-called cluster 6 is not comparable to cluster 1 in size; it is much smaller. Cluster 1 is a faint, loose association reminiscent of the Palomar clusters found in the outer halo of the Galaxy. It is useful to compare clusters 1 and 6 in more detail. Fig. 2 presents plots of the APM measures for two nearby areas of Fornax with the same stellar surface density as the region around cluster 6. Each area measures 4.3×4.3 arcmin^2, and both areas contain ~2300 stars. The top map shows cluster 6 and its surrounding area. Cluster 6 appears as a small concentration of stars near the centre. However, there also appear to be 'voids' of stars around it of approximately the same size. In the lower map, cluster 1 has been superposed on the data; it is seen as a much larger patch of stars in the lower left quadrant. Tests with the PLC technique have found this translated cluster 1 without difficulty. We therefore conclude that cluster 6 is not a cluster, and that it is simply caused by a statistical fluctuation of the stellar surface density in the field of Fornax (Section 3.6).

Strobel & Lake (1994), using the old photographic data of Hodge (1964a,b), could not confirm the presence or other-

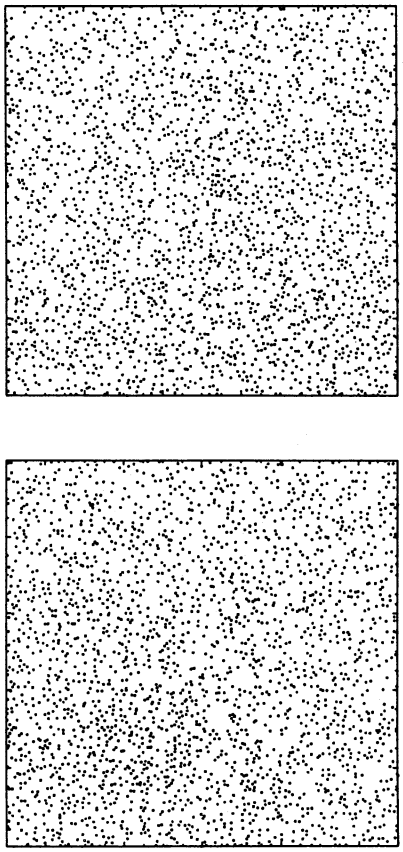

Figure 2. Comparison between cluster 6 and cluster 1 of Fornax. Maps made from APM measures of a deep CTIO 4-m plate. The limiting magnitude is $B_j \approx 23$; the size is 4.3×4.3 arcmin^2. The top map is centred on cluster 6. The lower map represents a nearby field of the same surface density; here cluster 1 has been added to the data, and it is easily seen as a denser patch in the lower left quadrant.

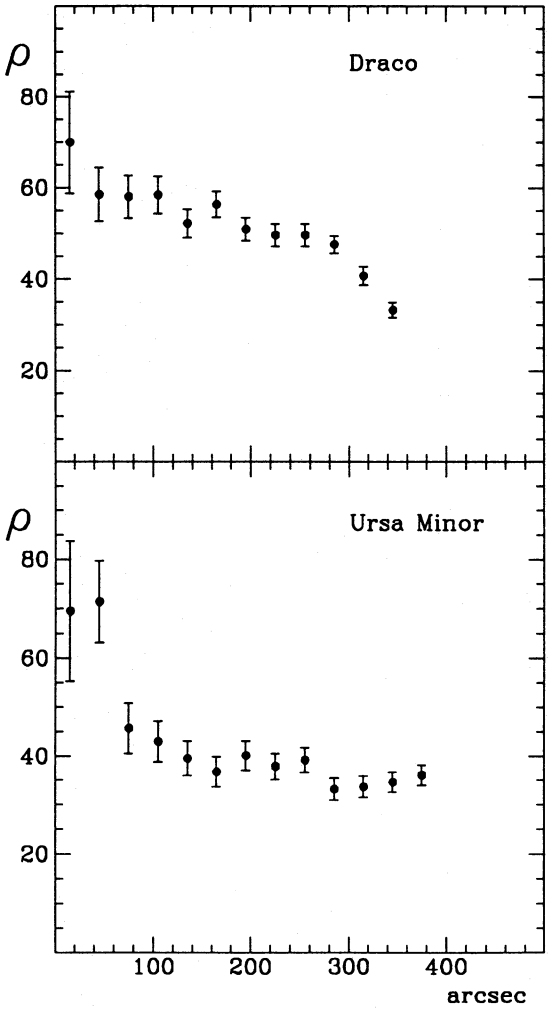

Figure 3. The stellar surface densities (stars per arcmin^2) for the core of Draco and Ursa Minor are shown as a function of the semi-major axis of the isopleths.

wise of a cusp of stars in the centre of Draco and Ursa Minor. Our identification of a non-random clump of stars at the centre of Ursa Minor (first reported by Olszewski & Aaronson 1985) prompted us to investigate the stellar distribution at the centre of these two galaxies in more detail. It is worth noting that the photographic data presented by Irwin & Hatzidimitriou (1993) do not go deep enough (and hence do not have sufficient spatial resolution) to reveal the Ursa Minor clump as a distinct component of the central density of Ursa Minor. What the photographic data confirm is that Ursa Minor is elongated into two large (several arcmin) concentrations of stars. We have used the morphological parameters given by Irwin & Hatzidimitriou (1993), namely, for Draco $\varepsilon = 0.29$ and the position angle of the major axis at $\theta = 82°$, and for Ursa Minor $\varepsilon = 0.56$ and $\theta = 53°$. Our CCD data are not suitable for determining these parameters, because they sample only the cores of these systems.

To the best that we can determine it (i.e. within 1 arcmin), the clump of stars, observed in Ursa Minor, is located at its centre. The diameter of the clump is roughly 2 arcmin or 40 pc. For both Draco and Ursa Minor, the exact position of the centre is not well defined from the CCD data. We investigated the most probable position of the centre by 'counting' stars, first in a grid covering the whole frame, and then in ellipses of the shape and orientation adopted above. To within the errors (~ 1 arcmin) the centres determined from the CCD data agree with those given by Irwin & Hatzidimitriou (1993). The surface stellar density radial profiles of Draco and Ursa Minor (number of stars per arcmin^2) are presented in Fig. 3. Stars were counted in annuli 30 arcsec wide, with shape and orientation as adopted above. The error bars reflect the number of stars in each bin. The points are plotted at the position of the average semimajor axis of the annuli. Draco shows a smooth increase of density towards the centre, with no obvious excess that could be attributable to a massive black hole. The density of Ursa Minor, however, shows a sudden increase within the first arcmin of its centre. The adopted shape of the isopleths is not critical; if one uses circular isopleths, the sudden increase near the centre of Ursa Minor is still quite obvious. Our observations show that there is a clear difference in the inner structure of Draco and Ursa Minor.

We can place a limit on the size of any putative central black hole for Draco and Ursa Minor, using the numerical

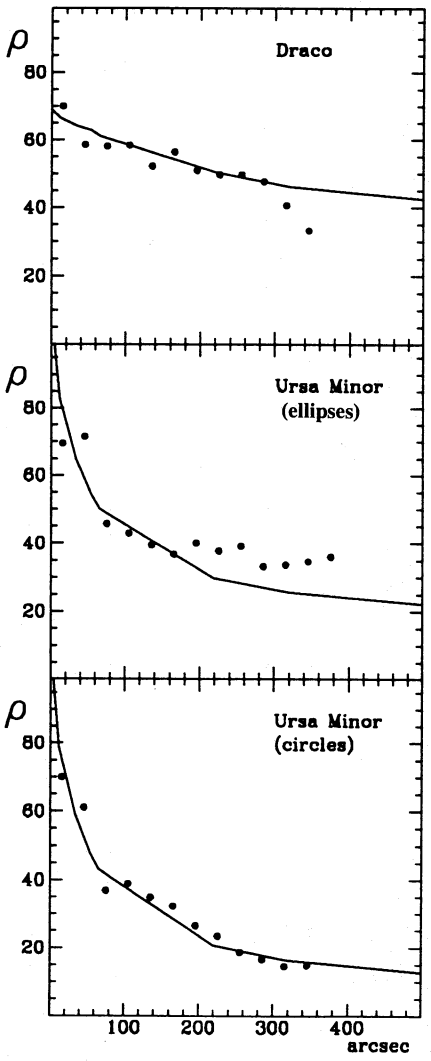

Figure 4. Young's (1980) models are fitted to the Draco and Ursa Minor stellar surface density. The adoption of circular isopleths for the central parts of UMi does not modify appreciably the density profile.

models described by Young (1980). The most recent estimates for the central velocity dispersion σ_v of Ursa Minor and Draco are 7.5 and 10 km s^{-1} (Hargreaves et al. 1994a,b). Assuming a canonical central mass density, ρ_o, of 1 $M_\odot$ pc^{-1} for both systems, we obtain core mass (equation 2 of Young 1980) estimates of $M_c = 3\times10^5$ $M_\odot$ for Ursa Minor, and 7×10^5 $M_\odot$ for Draco. The core mass, M_c, varies as $\rho_o^{-1/2}$ and σ_v^3. Hence M_c is relatively insensitive to the exact numerical factor used for the central mass density, but is strongly dependent on the velocity dispersion. Fits for central black hole models shown in Fig. 4 have a black hole mass of 3 M_c for Ursa Minor and 0.3 M_c for Draco. That is, any central black hole in Draco must be $<2\times10^5$ $M_\odot$, and $<9\times10^5$ $M_\odot$ in Ursa Minor.

The lack of any rising trend of observed velocity dispersion with decreasing central distance for either Draco or Ursa Minor (Strobel & Lake 1994; Hargreaves et al. 1994) would seem to corroborate these limits. Of course, the excess stars seen in the centre of Ursa Minor may well be simply a small stellar association/cluster rather than the cusp-like signature of a black hole. With a radius of only 1 arcmin (20 pc) distinguishing between these two possibilities, the use of radial velocities will prove very difficult. The most fruitful next step would be to obtain much deeper CCD data to enable the structure and photometry of the central region to be explored in more detail.

ACKNOWLEDGMENTS

This project has been supported financially, in part (SD), by the Natural Science and Engineering Research Council of Canada.

REFERENCES

Battinelli P., 1991, A&A, 244, 69
Battinelli P., Demers S., 1992, AJ, 104, 1458
Demers S., Irwin M. J., 1993, MNRAS, 261, 657
Demers S., Irwin M. J., Gambu I., 1994a, MNRAS, 266, 7
Demers S., Irwin M. J., Kunkel W. E., 1994b, AJ, 108, 1648
Eskridge P. B., 1988a, AJ, 96, 1336
Eskridge P. B., 1988b, AJ, 96, 1614
Faber S. M., Lin D. C. N., 1983, ApJ, 266, L17
Hargreaves J., Gilmore G., Irwin M. J., Carter D., 1994a, MNRAS, 269, 957
Hargreaves J., Gilmore G., Irwin M. J., Carter D., 1994b, MNRAS, 271, 693
Hodge P. W., 1961a, AJ, 66, 83
Hodge P. W., 1961b, AJ, 66, 249
Hodge P. W., 1964a, AJ, 69, 438
Hodge P. W., 1964b, AJ, 69, 853
Hodge P. W., 1969, PASP, 81, 875
Hodge P. W., 1971, ARA&A, 9, 35
Hodge P. W., Smith D. W., 1974, ApJ, 188, 19
Ibata R. A., Gilmore G., Irwin M. J., 1994, Nat, 370, 194
Irwin M. J., Hatzidimitriou D., 1993, in Smith G. H., Brodie J. P., eds, ASP Conf. Ser. Vol. 48, The Globular Cluster–Galaxy Connection. Astron. Soc. Pac., San Francisco, p. 322
Knapp G. R., Kerr F. J., Bowers P. F., 1978, AJ, 83, 360
Kunkel W. E., 1979, ApJ, 228, 718
Lee M. G., Freedman W., Mateo M., Thompson I., Roth M., Ruiz M.-T., 1993, AJ, 106, 1420
Lynden-Bell D., 1967, MNRAS, 136, 101
Lynden-Bell D., 1982, Observatory, 102, 202
Majewski S. R., 1993, in Majewski S. R., ed., ASP Conf. Ser. Vol. 49, Galaxy Evolution: The Milky Way Perspective. Astron. Soc. Pac., San Francisco, p. 5
Mighell K. J., 1990, A&AS, 82, 1
Mould J., Aaronson M., 1983, ApJ, 273, 530
Mould J. R., Bothum G. D., Hall P. J., Staveley-Smith L., Wright A. E., 1990, ApJ, 362, L55
Nemec J. M., Whelau A., Mendes de Oliveira C., 1988, AJ, 96, 528
Olszewski E. W., Aaronson M., 1985, AJ, 90, 2221
Silk J., Wyse R. F. G., 1993, Phys. Rep., 231, 293
Stetson P. B., 1979, AJ, 84, 1149
Strobel N. V., Lake G., 1994, ApJ, L83
van de Rydt F., Demers S., Kunkel W. E., 1991, AJ, 102, 130
Verner G., Demers S., Hardy E., Kunkel W. E., 1981, AJ, 86, 357
Young P., 1980, ApJ, 242, 1232